

Introduction of Damping, Synchronizing and Inertial Effects using Controlled Power Injection Devices

Kaustav Dey, P. Agnihotri, A. M. Gole *Fellow, IEEE* and A. M. Kulkarni *Member, IEEE*

Abstract—This paper presents a theoretical study of damping, synchronizing and inertial control laws, implemented using controllable power injection devices like HVdc, FACTS or renewable-energy/storage systems which have power-electronic grid interfaces. The approach is to use a simplified dynamical model of a power system to arrive at generalized results regarding the effect of the strategies on the electro-mechanical dynamics of the system. These results are not dependent on the size, network topology and operating condition of the power system. This paper presents a differential-algebraic formulation and generalized eigenvalue analysis to facilitate a unified study of the effects of the control laws on the electro-mechanical modes. The damping, synchronizing and inertial control laws can themselves be extended to include the possibility of mutual-damping, synchronizing and inertial effects when multiple devices are present. The control laws are not only simple and intuitive, but are found to have a predictable and generally beneficial impact on the electro-mechanical dynamics of the grid, even when detailed models are considered.

Index Terms—High Voltage direct current(HVdc), Power System Control, Dynamic Stability, Inertia Emulation.

I. INTRODUCTION

The advent of four technologies: (a) Renewable-Energy Systems, (b) Energy Storage Systems, (c) Large rating Voltage Source Converter (VSC) based power-electronic systems and (d) Wide-Area Measurement Systems (WAMS) [1] is expected to have a major impact on the operation, control and dynamics of power systems. The integration of a large number of distributed energy sources in a large synchronous grid can be facilitated by a flexible AC transmission(FACT) network with rapidly controllable power flows and injections. The control of power flows and injections is necessary to avoid electro-mechanical stability problems. VSCs are suitable actuators for implementing these control strategies as they can provide fast and independent control of real and reactive power. Moreover, VSCs are being increasingly used as dc-ac grid interfaces for not only renewable-energy and storage systems, but for some FACTS and HVdc systems as well. The measurements from WAMS can provide non-local feedback or supervisory signals to enhance these stability controllers [1].

Electro-mechanical stability of a synchronous grid may be classified as follows:

1) Angular stability: This involves the relative motion between the rotors of the synchronous machines. This motion is

generally oscillatory for small disturbances (“swing modes”). The damping of these swings is generally a major concern. Large disturbance stability of relative motion is also a concern, as synchronous generators may lose synchronism due to large disturbances like faults if the transmission system is weak or stressed.

2) Frequency stability: This refers to the common, or centre-of-inertia(COI) movement of the rotors of the synchronous machines. This motion is dependent on the cumulative load-generation-(asynchronous export/import) balance within the synchronous grid and the cumulative inertia.

The frequency at any location consists of both the common motion component as well as relatively fast-changing components due to the swings between synchronous machines. In a large power system, local inertia and local power-imbalance play a role in short-term frequency dynamics, before the frequency disturbance propagates like a wave [2] to the rest of the system.

While the problem of electro-mechanical stability improvement can be thought of as just another control system design problem, the large size, complexity, non-linearity and uncertainties associated with a power system makes it difficult to take a purely numerical approach to controller design and optimization. We require the controller to have attributes like (a) design simplicity, (b) few parameters, (c) robustness and predictable behaviour under different network topology and operating conditions, and (d) robustness to loss of communication if non-local feedback signals are used. This motivates us to look for special strategies and controller structures in a *top-down* fashion, based on an analytical rather than a numerical approach. Unfortunately, given the difficulty in deriving analytical results with detailed power system models, this initial search has to use only the simplest of models of the power system (synchronous generators modelled by the classical model and a lossless ac network). The expectation is that the simplified analysis should suggest the controllers (i.e. the control laws and feedback signals) with the attributes listed above, which can then be fine-tuned/improved for real-life application.

The key general results which can be derived by the examination of the eigenstructure/eigenspectrum of the simplified model of a power system are as follows:

(1) Real shunt power modulation in proportion to the local bus frequency improves the damping of *all* the controllable swing modes. Note that shunt power injection can be achieved through controllable loads [3], power-electronically controlled renewable-energy systems [4] and energy storage systems [5].

(2) HVdc power flow modulation in proportion to the

Kaustav Dey and A. M. Kulkarni are with the Department of Electrical Engineering, Indian Institute of Technology, Bombay, India.

P. Agnihotri and A. M. Gole are with the Department of Electrical and Computer Engineering, University of Manitoba, Canada. email: anil@ee.iitb.ac.in

difference in bus frequencies at the two terminals produces similar damping effect.

(3) Reciprocal power injection control of multiple power modulation-capable devices using symmetric positive definite proportional gain matrices and the frequency signals at these locations can also produce damping.

Results (1) and (2) are quite intuitive and have been derived in the earlier literature in various forms [3], [6]–[8]. A non-obvious fact is that introduction/enhancement of damping by these control laws is not dependent on the network size, topology, operating condition, the number of generators and the location of the devices, although the amount of damping influence exerted by the controllers will depend on these factors. The damping effect is also experienced by all the controllable swing modes. Result (3) has been reported recently in the literature [6], [9].

Although simple models are used for the derivation of these laws, numerical experiments carried out earlier [6], [8] have reported that these control laws produce the expected damping effect even when detailed models of a power system are considered. While similar control laws for controllable shunt reactive power injections have also been derived using simplified models (the preferred feedback signal being the derivative of the voltage magnitude), the behaviour is significantly different when detailed models are considered [8]. This explains why we consider only controllable real power injections by shunt connected devices in this paper.

Introduction of “synchronizing” and “inertial” effects by replacing the frequency signal by the phase angle and rate-of-change of frequency respectively, seems to be a logical extension to the damping control laws mentioned earlier. However, it remains to be seen whether the effect on the electro-mechanical modes can be generalized in a similar fashion as the results of the damping control laws.

In this paper, we extend the results (1)-(3) to cover synchronizing and inertial effects introduced by proportional control laws based on phase angular differences and rate-of-change of frequency respectively. To facilitate this, we introduce a structure-preserving formulation of the linearized differential-algebraic equations of the system, so that the changes in the eigenstructure/eigenspectrum due to the application of the damping/synchronizing/inertial control by power injection devices at any bus (not necessarily a generator bus), is clearly revealed. A generalized eigenvalue sensitivity formulation of these differential-algebraic equations is used to characterize the influence of damping/synchronizing/inertial control on the swing modes. The effect of the synchronizing and inertial control is also characterized in terms of the amplitude of relative angular and frequency deviations following disturbances like faults and load/generation trippings respectively. Therefore, the main contribution of this paper is to generalize the results available in prior literature and present a unified analysis of the strategies. Case studies on a detailed model of a large grid corroborate the inferences drawn from the analysis of a simplified power system model.

The effect of the various control strategies can be intuitively understood by using a circuit analogy of the electro-mechanical system [9], [10]. The circuit analogy also draws

our attention to various possibilities like mutually-induced damping and synchronizing effects. Therefore, before proceeding for a more formal state-space analysis, we examine (in Section II) the control strategies using this analogous model. Section III introduces the generalized formulation, which reveals the eigenstructure and facilitates the eigenvalue sensitivity analysis. Section IV presents a discussion on some of the practical issues relating to real-life implementation of the control laws, while Section V presents case studies on detailed models, which validate the inferences drawn from the simplified model.

II. CIRCUIT ANALOGY OF ELECTRO-MECHANICAL SYSTEM

A circuit analogy of the electro-mechanical system [9], [10] can be constructed if we assume the following:

- 1) Synchronous generators are represented as voltage sources behind transient reactances (classical model).
- 2) Generator mechanical power input and load power are assumed to be constant.
- 3) All transmission lines are assumed to be lossless.
- 4) The phase angular differences between buses are small.
- 5) All bus voltages are assumed to be 1 p.u.
- 6) The controlled power injection devices have negligible response time.

TABLE I: List of Symbols

Abbreviation	Description of variable
δ_g	Generator Rotor angle (in rad)
δ_b	Bus voltage phase angle (in rad)
ω_g	Generator Rotor speed (in rad/s)
ω_b	Bus voltage frequency (in rad/s)
ω_B	Machine base speed (in rad/s)
H	Generator inertia constant (in s)
P_e	Power injected by generator (in p.u.)
P_{sh}	Shunt injected real power (in p.u.)
P_{dc}	HVdc link power flow (in p.u.)
P_{ser}	Series injected real power (in p.u.)
V	Bus voltage magnitude (in p.u.)
V_R	Series injected reactive voltage (in p.u.)
I	Line current magnitude (in p.u.)
ζ	Line current phase angle (in rad)
I_R	Shunt injected reactive current (in p.u.)

Since the transmission system is assumed to be lossless, we can associate a power flow with each branch in the same way as a current. Moreover, in any loop in the system, the sum of phase angular differences across the branches is zero. Thus we can use the following analogies:

Power flow through a branch \iff Current.

Time derivative of bus voltage phase angle \iff Voltage. Using these analogies, the electro-mechanical system can be represented by an analogous circuit. The inertia of a synchronous generator is analogous to a capacitor because:

$$\frac{2H}{\omega_B} \frac{d\Delta\omega_g}{dt} = \mathcal{C} \frac{d\Delta\omega_g}{dt} = -\Delta P_e \quad (1)$$

Similarly, a transmission line/transformer branch whose reactance is x_{ij} is analogous to an inductor since,

$$\frac{d(\Delta\phi_{ij})}{dt} = \mathcal{L} \frac{d\Delta P_{ij}}{dt} \quad (2)$$

where $\mathcal{L} = x_{ij}$, since $\Delta P_{ij} \approx \frac{\Delta\phi_{ij}}{x_{ij}}$.

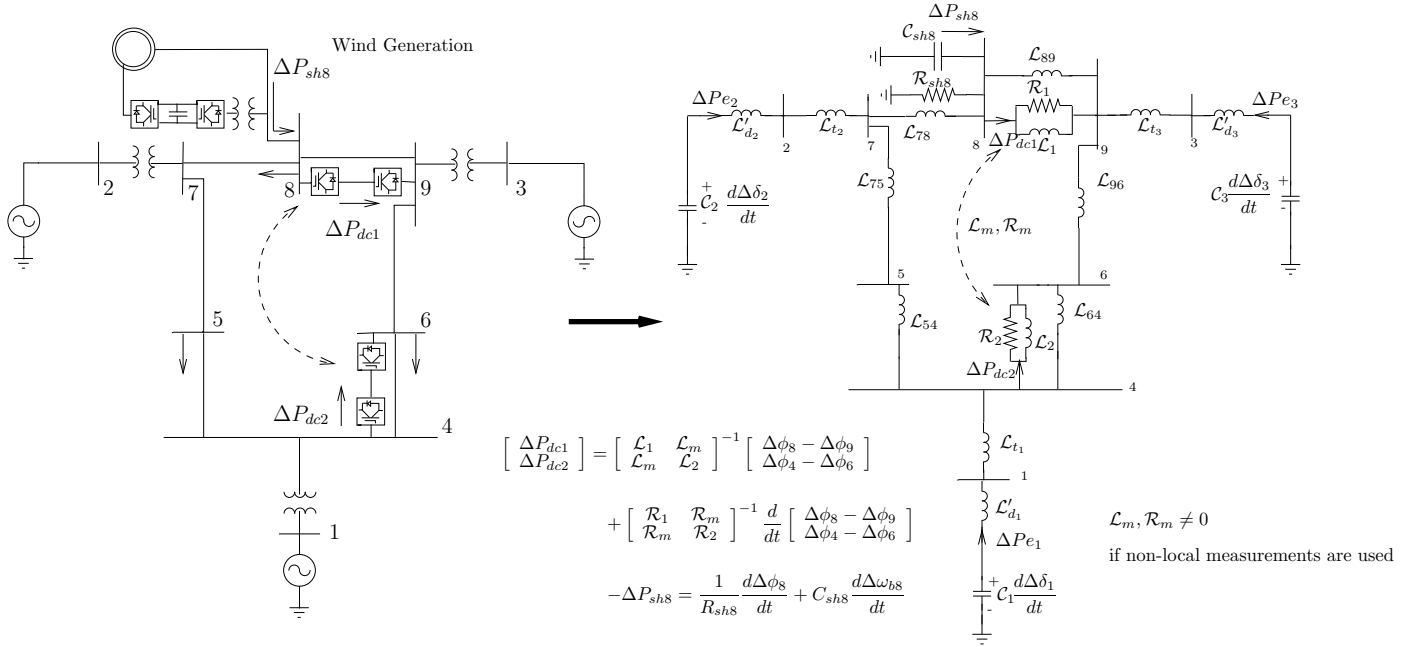


Fig. 1: Circuit analogy of an electro-mechanical system with controllable power injections using dc links and a shunt connected device

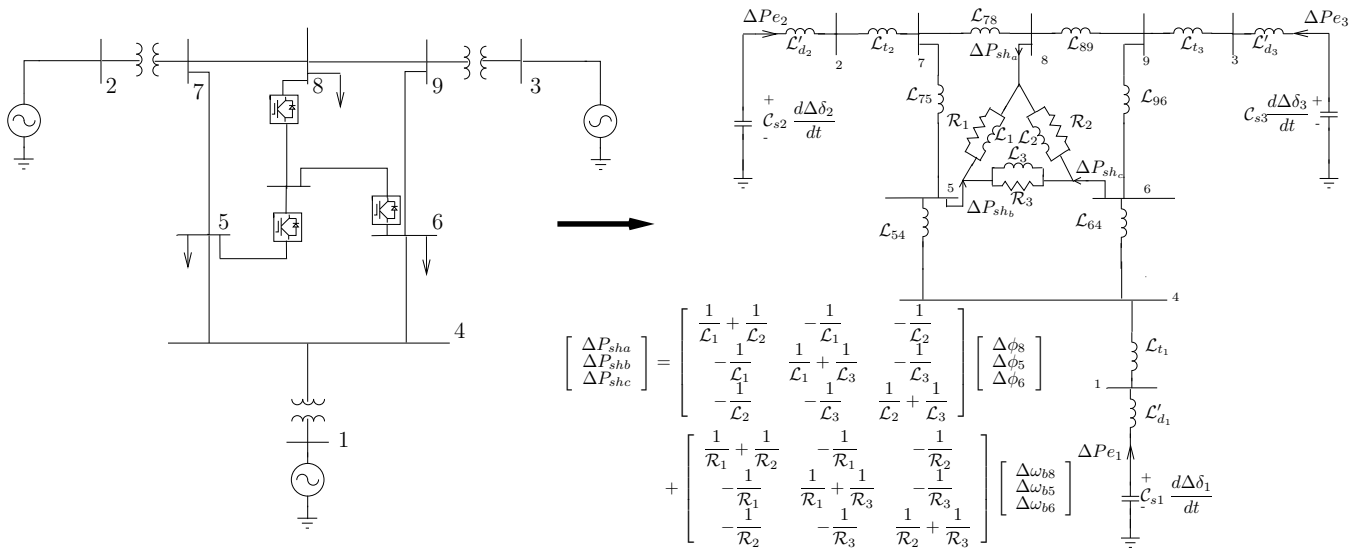


Fig. 2: Control Strategy for an embedded three-terminal MTdc Link

A. Control Strategies

The main utility of the circuit analogy is that it provides a clue to the control strategy to improve stability with, say, a dc link or a shunt connected renewable or energy storage system - see Fig. 1. It shows two VSC-based dc links connected between bus pairs (8,9) and (4,6). The system also has a shunt energy storage (wind generator) connected to bus 8.

If power flow of the dc link is controlled in proportion to the derivative of the voltage phase angular difference between the buses (i.e., the bus frequency difference), a dc line behaves like a resistance \mathcal{R} in the analogous circuit. This introduces damping with a simple local strategy.

If power flow in a dc link is controlled in proportion to the voltage phase angular difference between the buses to

which it is connected, then a dc line behaves like an AC line, i.e., the effect is the addition of another inductive link \mathcal{L} in the analogous circuit. This is expected to reduce angular deviations following disturbances (synchronizing effect).

If shunt power withdrawal is controlled in proportion to the rate of change of frequency of the bus by a renewable-energy source or an energy storage system or a controllable load, then the effect is addition of a capacitive link \mathcal{C} in the analogous circuit as shown in Fig. 1. This enhances the system inertia.

There are certain advantages of these strategies:

- a) the strategies are simple and use local measurements.
- b) the introduction of “resistive” and “inductive” links will always enhance damping and synchronizing effects respectively, for all swing modes in the system (except for

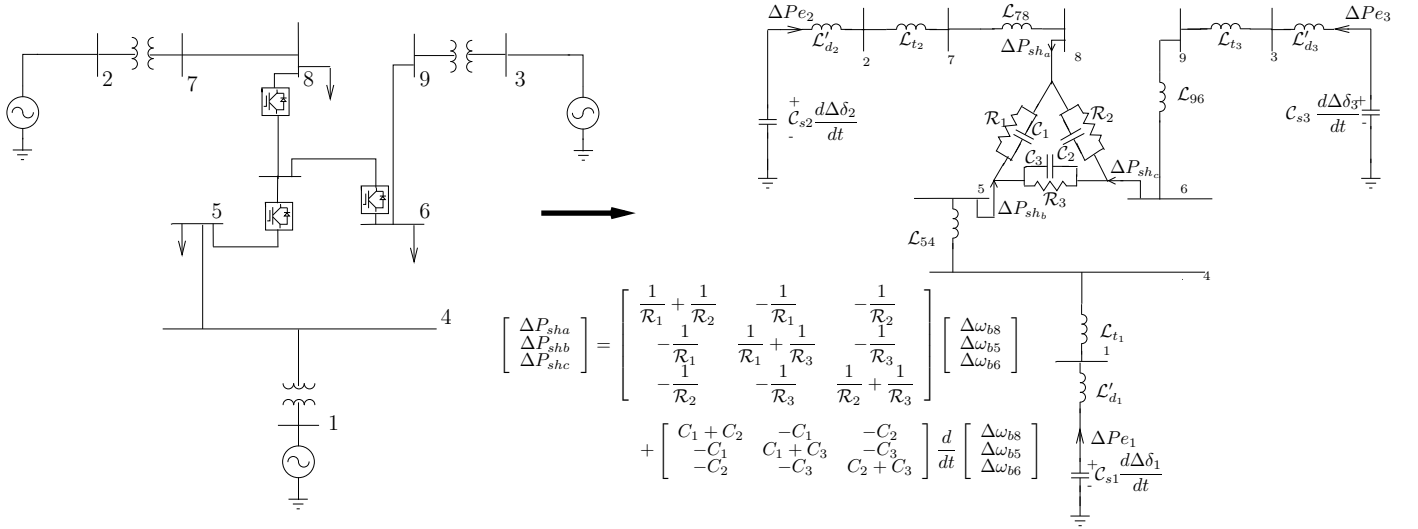


Fig. 3: Control Strategy for an asynchronous MTdc Link

those modes which are not observable in the phase angular difference at the dc link location or in the bus frequency at the shunt power injection device location).

c) Shunt capacitive elements will increase the cumulative inertia and will affect the common-mode motion of the electro-mechanical system. Although it is also possible to have dc link power controlled so as to introduce series-branch capacitive effects, this will not affect the common-mode motion as there is no net change in the cumulative load-generation balance. However, this may boost local inertia by the transfer of power from other locations.

d) Where multiple actuators are present, the same strategies may be applied for each of them (more resistors/inductors/capacitors get added in the circuit); their independent actions are not adversarial.

e) The controller gains determine the value of the resistors, inductors and capacitors introduced by the control strategy. As the gain is increased from zero to infinity, the resistor and inductor values decrease from infinity to zero and capacitors increase from zero to infinity. At large gains, the links essentially short circuit the branches across which they are connected. This implies that these effects will not monotonically increase with increasing gain, as discussed in [5].

B. Emulation of Mutual effects

The circuit analogy also suggests the possibility of emulating mutual inductance and resistance which are indicated using a dashed arrowhead line in Fig. 1. Here, the controller at each location uses local and specific non-local measurements. The gain matrix involving self and mutual terms are shown in Fig. 1. The condition under which this control becomes useful and robust to communication failure is when the gain matrices are symmetric positive definite [6].

C. Multi Terminal dc links

The circuit analogy helps us to understand the effect that can be achieved using power modulation in a Multi Terminal

dc(MTdc) link. Let us consider a MTdc system connected across buses 5, 6 and 8 as shown in Fig. 2. The power injection at each of the terminals is controlled using functions of bus voltage phase angle at the individual terminals. The analogous circuit for the MTdc link is also shown in Fig. 2.

D. Asynchronous dc links

In asynchronous grids interconnected by dc links, the emulation of inertial and damping effects as shown in Fig. 3, allows the neighbouring asynchronous grids to come to the assistance of a grid which is faced with a sudden load-generation imbalance.

Another theoretical possibility is the variation of power drawal by a shunt connected device in proportion to the phase angle deviations at a bus. This is like connecting an inductor in shunt in the analogous circuit, and will mimic integral control of frequency (like isochronous governors [11]).

III. GENERALIZED EIGENVALUE SENSITIVITY ANALYSIS

The small signal model of a power system is derived using the real and reactive power balance equations as given in [8]. As before, we consider the classical model of a synchronous machine, assume a lossless network, but relax the assumption that all bus voltage magnitudes are 1 p.u. Moreover, dependence of load power on voltage is allowed. The model can then be written in *differential-algebraic* form as follows:

$$\mathcal{M}_u \dot{x}_u = A_u x_u + B_u u_{in} \quad (3)$$

where x_u and u_{in} are respectively as follows

$$x_u^T = [\Delta\delta_g^T, \Delta\delta_b^T, \Delta\omega_g^T, \Delta\omega_b^T, \Delta V^T, \Delta I^T, \Delta\zeta^T] \quad (4)$$

$$u_{in}^T = [0^T, 0^T, 0^T, \Delta P_{sh}^T, \Delta I_R^T, \Delta V_R^T, \Delta P_{ser}^T] \quad (5)$$

0 denotes a zero vector of appropriate dimension. The block matrices \mathcal{M}_u , A_u and B_u can be represented as follows

$$\mathcal{M}_u = \begin{bmatrix} I & 0 & 0 \\ 0 & M & 0 \\ 0 & 0 & 0 \end{bmatrix}, A_u = \begin{bmatrix} 0 & I & 0 \\ -A_1 & 0 & -A_2 \\ -A_2^T & 0 & -A_3 \end{bmatrix}, B_u = I \quad (6)$$

where I and 0 represent identity matrices and zero matrices of appropriate dimensions, $M = \text{diag}(2H_i/\omega_B, 0)$. The partitioning of \mathcal{M}_u and A_u into block matrices is consistent with the partitioning of the variables x_u and u_{in} (indicated by dashed lines as given above).

Note that $A_1 = A_1^T$ and $A_3 = A_3^T$ because of the assumptions (1) to (4) of Section II - see the derivation of the individual terms from the linearized real and reactive power equations in [8].

ΔV_R , ΔP_{ser} , ΔI_R are inputs which can be varied with actuators like TCSC/SSSC, SSSC, and STATCOM/SVC respectively. We limit our analysis in this paper to the study of real power flow or shunt real power injection devices only. Hence, ΔP_{sh} is taken to be the only non-zero input. Thus, the variables ΔV , ΔI , $\Delta \zeta$ can be eliminated and we get the reduced order model:

$$\mathcal{M}\dot{x} = Ax + \mathcal{B}u_{in} \quad (7)$$

$$\mathcal{M} = \begin{bmatrix} I & 0 \\ 0 & M \end{bmatrix}, \mathcal{A} = \begin{bmatrix} 0 & I \\ -A_r & 0 \end{bmatrix}, \mathcal{B} = \begin{bmatrix} I & 0 & 0 \\ 0 & I & B_r \end{bmatrix} \quad (8)$$

where $A_r = A_1 - A_2A_3^{-1}A_2^T$ and $B_r = -A_2A_3^{-1}$. Note that A_r is symmetric. The state variables of the reduced model are

$$x^T = \begin{bmatrix} \Delta\delta_g^T & \Delta\delta_b^T & \Delta\omega_g^T & \Delta\omega_b^T \end{bmatrix} = \begin{bmatrix} \Delta\delta^T & \Delta\omega^T \end{bmatrix} \quad (9)$$

Let v_i and u_i be the right and left generalized eigenvectors respectively, of the generalized eigenvalue λ_i of the matrix pair $(\mathcal{A}, \mathcal{M})$. The eigenvectors can be partitioned as follows:

$$v_i^T = \begin{bmatrix} v_{\delta gi}^T & v_{\delta bi}^T & v_{\omega gi}^T & v_{\omega bi}^T \end{bmatrix} = \begin{bmatrix} v_{\delta i}^T & v_{\omega i}^T \end{bmatrix} \quad (10)$$

$$u_i^T = \begin{bmatrix} u_{\delta gi}^T & u_{\delta bi}^T & u_{\omega gi}^T & u_{\omega bi}^T \end{bmatrix} = \begin{bmatrix} u_{\delta i}^T & u_{\omega i}^T \end{bmatrix} \quad (11)$$

A. Eigenstructure and Eigenspectrum

The generalized eigenvectors corresponding to the generalized eigenvalue λ_i of the matrix pair $(\mathcal{A}, \mathcal{M})$ satisfy the following relations:

$$\mathcal{A}v_i = \lambda_i \mathcal{M}v_i, \quad u_i^T \mathcal{A} = \lambda_i u_i^T \mathcal{M} \quad (12)$$

Using \mathcal{A} and \mathcal{M} as given in (8), we get

$$\lambda_i^2 M v_{\delta i} = A_r v_{\delta i}, \quad \lambda_i^2 M u_{\omega i} = A_r u_{\omega i} \quad (13)$$

Using (13), we can say that both $v_{\delta i}$ and $u_{\omega i}$ are right eigenvectors of the matrix pair (A_r, M) corresponding to eigenvalue λ_i^2 . Hence, for any arbitrary non-zero scalar h_i ,

$$u_{\omega i} = h_i v_{\delta i} \quad (14)$$

Using (12) and (14), the following relations can be derived

$$v_{\omega i} = \lambda_i v_{\delta i}, \quad u_{\delta i} = \lambda_i M u_{\omega i} \quad (15)$$

$$v_i^T = \begin{bmatrix} v_{\delta i}^T & \lambda_i v_{\delta i}^T \end{bmatrix}, u_i^T = \begin{bmatrix} \lambda_i h_i (M v_{\delta i})^T & h_i v_{\delta i}^T \end{bmatrix} \quad (16)$$

In addition note that,

(a) A_r is generally negative semi-definite for normal operating conditions. A_r is singular because real and reactive power flows are functions of phase angular differences.

(b) For a system having n_g number of synchronous generators and n_b number of buses, A_r and M are both of size

$(n_b + n_g) \times (n_b + n_g)$. Hence, the matrix pair (A_r, M) will have $(n_b + n_g)$ generalized eigenvalues.

(c) Since M is a diagonal matrix and has n_b zero diagonal entries, the number of infinite eigenvalues of (A_r, M) will be n_b [12]. The remaining n_g eigenvalues correspond to the electro-mechanical modes, with $(n_g - 1)$ eigenvalues corresponding to swing modes and a zero eigenvalue corresponding to the centre-of-inertia motion.

(d) As A_r is symmetric negative semi-definite while M is symmetric positive semi-definite, the finite eigenvalues will be real and ≤ 0 .

(e) The square roots of the generalized eigenvalues of (A_r, M) are the generalized eigenvalues of $(\mathcal{A}, \mathcal{M})$. Hence, from the eigenspectrum of (A_r, M) , it can be inferred that $(\mathcal{A}, \mathcal{M})$ will have

- two zero eigenvalues which represent the centre-of-inertia (COI) motion.
- $2(n_g - 1)$ complex conjugate finite non-zero eigenvalues corresponding to $(n_g - 1)$ swing modes.
- $2n_b$ infinite eigenvalues. The infinite eigenvalues have no physical significance, as they can be excited only by initial conditions which violate the algebraic power balance equations at a node.

These results are valid if all the synchronous generators are synchronously connected. If the network has k asynchronous areas, $(\mathcal{A}, \mathcal{M})$ will have $2k$ zero eigenvalues corresponding to COI motion of each area. Having analyzed the eigenspectrum of the matrices, we now analyze the effect of the different control strategies.

B. Damping Control

Consider a single HVdc link be connected between bus r and bus s where the power flow is controlled in proportion to the bus voltage frequency difference. Therefore,

$$\Delta P_{shr} = -\frac{(\Delta\omega_{br} - \Delta\omega_{bs})}{\mathcal{R}_{rs}}, \Delta P_{shs} = \frac{(\Delta\omega_{br} - \Delta\omega_{bs})}{\mathcal{R}_{rs}} \quad (17)$$

Note that the controller gain is $\frac{1}{\mathcal{R}_{rs}}$. This strategy will cause a perturbation in four terms of \mathcal{A} ($2, 2$) block. This is a symmetric negative semi-definite perturbation of A_r if $\mathcal{R}_{rs} > 0$.

The perturbation of an eigenvalue λ_i for a small gain (large value of R_{rs}) is obtained using (45), and is given by:

$$\Delta\lambda_i = \frac{\begin{bmatrix} u_{\omega bi}(r) & u_{\omega bi}(s) \end{bmatrix} \begin{bmatrix} -\frac{1}{\mathcal{R}_{rs}} & \frac{1}{\mathcal{R}_{rs}} \\ \frac{1}{\mathcal{R}_{rs}} & -\frac{1}{\mathcal{R}_{rs}} \end{bmatrix} \begin{bmatrix} v_{\omega bi}(r) \\ v_{\omega bi}(s) \end{bmatrix}}{2\lambda_i h_i v_{\delta i}^T M v_{\delta i}} \quad (18)$$

$$= \frac{\begin{bmatrix} v_{\delta bi}(r) & v_{\delta bi}(s) \end{bmatrix} \begin{bmatrix} -\frac{1}{\mathcal{R}_{rs}} & \frac{1}{\mathcal{R}_{rs}} \\ \frac{1}{\mathcal{R}_{rs}} & -\frac{1}{\mathcal{R}_{rs}} \end{bmatrix} \begin{bmatrix} v_{\delta bi}(r) \\ v_{\delta bi}(s) \end{bmatrix}}{2v_{\delta i}^T M v_{\delta i}} \quad (19)$$

where, $u_{\omega bi}(r)$, $v_{\delta bi}(r)$ and $v_{\omega bi}(r)$ denote the r^{th} entries of $u_{\omega bi}$, $v_{\delta bi}$ and $v_{\omega bi}$ respectively.

Note that $v_{\delta i}$ can be chosen to be real, λ_i is purely imaginary and finite and $v_{\delta i}^T M v_{\delta i} > 0$ for the swing modes. Therefore if $\mathcal{R}_{rs} > 0$ and $v_{\delta bi}(r) - v_{\delta bi}(s) \neq 0$, then the eigenvalue perturbation is real and negative, indicating the improvement

of damping. If $(v_{\delta bi}(r) - v_{\delta bi}(s) = 0)$ for some i , it means that the mode is not observable in the frequency difference signal at the dc link location, and therefore, the corresponding mode is unaffected. An interesting result proved in [8] is that non-observability of a swing mode in the bus frequency difference signal at a particular location also implies non-controllability of that mode using power flow control at that location.

In case of non-local feedback signals from multiple dc links, the corresponding diagonal and off-diagonal entries of $\mathcal{A}(2, 2)$ will be modified. If shunt real power drawal in proportion to the corresponding bus frequency variation using a single shunt connected device is considered, then only one diagonal term in $\mathcal{A}(2, 2)$ will be affected. In general, the damping control strategy should introduce a symmetric negative definite or semi-definite perturbation in $\mathcal{A}(2, 2)$ to ensure that there is a positive damping influence on all the controllable modes.

C. Synchronizing and Inertial Control

Similar results can be derived for inertial control and synchronizing control. The only difference between damping control and synchronizing control (i.e., power flow in proportion to phase angular difference) of a dc link is that the sub-matrix A_r of \mathcal{A} is affected instead of $\mathcal{A}(2, 2)$ block. The perturbation in eigenvalue λ_i is obtained as follows:

$$\Delta\lambda_i = \frac{\begin{bmatrix} v_{\delta bi}(r) & v_{\delta bi}(s) \end{bmatrix} \begin{bmatrix} -\frac{1}{\mathcal{L}_{rs}} & \frac{1}{\mathcal{L}_{rs}} \\ \frac{1}{\mathcal{L}_{rs}} & -\frac{1}{\mathcal{L}_{rs}} \end{bmatrix} \begin{bmatrix} v_{\delta bi}(r) \\ v_{\delta bi}(s) \end{bmatrix}}{2\lambda_i v_{\delta i}^T M v_{\delta i}} \quad (20)$$

Therefore, the frequencies of the controllable swing modes are increased if $\mathcal{L}_{rs} > 0$.

Inertial control will affect \mathcal{M} . Hence, the eigenvalue sensitivity expression of (49) should be used. The introduction of an inertial effect at bus r , using a shunt power injection device causes an eigenvalue perturbation (for a gain $C_r \geq 0$) which is

$$\Delta\lambda_i = -\lambda_i \frac{v_{\delta bi}(r) C_r v_{\delta bi}(r)}{2v_{\delta i}^T M v_{\delta i}} \quad (21)$$

For a swing mode, this means that the modal frequency will reduce. The introduction of an inertia will also cause an additional swing mode to be created since the number of non-zero eigenvalues in M will increase by one. Moreover, the initial rate of change of COI frequency for a sudden load-generation imbalance will reduce since the cumulative inertia of the system increases.

When multiple devices are present, a ‘‘mutual strategy’’ using matrix gains may be used, in which case C_r is a matrix. In general, swing mode frequencies will either reduce or remain unchanged if C_r is symmetric positive semi-definite.

The introduction of inertia and synchronizing effects at first glance seems mutually adversarial in the small-signal sense as one strategy increases the swing mode frequency while the other reduces it. This aspect is examined more closely in the next subsection.

D. Effects of Synchronizing and Inertial Control under various disturbances

While synchronizing control increases the frequency of the swing modes, this by itself does not seem to be of use. However, the implications of this for large disturbance stability (loss of synchronism) needs further analysis. A synchronous grid can be expected to remain in synchronism after a disturbance if it can convert the kinetic energy gained during a large disturbance to potential energy [10]. This aspect is related to the maximum angular deviation which is experienced after the disturbance, since power flows depend non-linearly on the phase angular differences. While it is very difficult to analyze the non-linear model of the system for evaluating the deviations, a few inferences relating to the maximum angular deviations following disturbances can be obtained from a linearized model. This analysis is admittedly very approximate as it is based on a linearized model, but serves as a useful pointer to the effect of synchronizing control. The key additional assumptions are:

- the disturbance excites only one dominant swing mode.
- the introduction of the control strategy does not modify the mode-shape of the controllable swing mode appreciably.

Note that in the analysis, the matrices and deviations of the angles and speeds are with respect to the post-disturbance equilibrium.

We attempt to answer the question: Do symmetric negative semi-definite perturbations to A_r always ensure that the amplitude of modal angular deviations does not increase after disturbances like a fault? In this context, it is useful to note that

$$\Delta\omega^T M \Delta\omega - \Delta\delta^T A_r \Delta\delta = \text{constant} \quad (22)$$

If the disturbance is a fault, we assume that the system primarily gains kinetic energy during the fault-on period. After fault clearing,

$$\Delta\omega(0)^T M \Delta\omega(0) = \Delta\omega(t)^T M \Delta\omega(t) - \Delta\delta(t)^T A_r \Delta\delta(t) \quad (23)$$

where $\Delta\omega(0)$ is the speed deviation at the fault clearing time. If only one dominant swing mode is excited due to the disturbance, thereby implying a sinusoidal oscillation, then

$$\Delta\delta(t) = k_\delta \sin(\Omega_i t + \phi) v_{\delta i} \quad (24)$$

where k_δ is the amplitude of the modal angular deviation and Ω_i is the angular frequency of the excited mode. Since the eigenvector $v_{\delta i}$ can be chosen to be real, all the angular deviations will reach their maximum (positive or negative) at the same time instant. At the time instant of the maximum angular deviations,

$$\begin{aligned} \Delta\omega(0)^T M \Delta\omega(0) &= -\Delta\delta_{max}^T A_r \Delta\delta_{max} & (25) \\ &= -k_\delta^2 v_{\delta i}^T A_r v_{\delta i} & (26) \end{aligned}$$

$\Delta\delta_{max}$ denotes the vector of angular deviations when the amplitudes are maximum and the kinetic energy is zero. If the synchronizing control as discussed in the previous section is introduced, then A_r is perturbed by a symmetric negative

semi-definite matrix. Since we have assumed that the mode-shape of this mode (i.e., the right eigenvector) is not significantly changed due to the introduction of the synchronizing control, the relative observability of the mode in the states remain unchanged. Therefore, if the maximum amplitude of the modal angle of the modified system is k'_δ , then

$$\Delta\omega(0)^T M \Delta\omega(0) = -k'^2_\delta v_{\delta i}^T (A_r + \Delta A_r) v_{\delta i} \quad (27)$$

From (26) and (27) and using the fact that ΔA_r and A_r are symmetric negative semi-definite, it can be inferred that

$$-k'^2_\delta v_{\delta i}^T A_r v_{\delta i} \leq -k^2_\delta v_{\delta i}^T A_r v_{\delta i} \quad (28)$$

Hence, it is clear from (28) that $|k'_\delta| \leq |k_\delta|$ implying either reduction or no change in the amplitude of the modal angular deviation for a disturbance like fault, which is beneficial.

For inertial control action it is well known that if the cumulative inertia increases then the rate-of-change of COI frequency will be smaller. However, the effect on relative frequencies in the grid also needs to be examined. The question is: Do symmetric positive semi-definite perturbations to the M matrix always ensure that the amplitude of relative speed oscillations does not increase after a load/generation tripping?

If the disturbance is a generator or load outage, then the pre-disturbance and post-disturbance relative speeds at equilibrium are the same, but the equilibrium values of the relative angles do change. Hence the system primarily sees a initial jump in potential energy when a load or generator is tripped. Therefore,

$$-\Delta\delta(0)^T A_r \Delta\delta(0) = \Delta\omega(t)^T M \Delta\omega(t) - \Delta\delta(t)^T A_r \Delta\delta(t) \quad (29)$$

where $\Delta\delta(0)$ is the angular deviation at the instant of outage. At the instant of maximum modal speed deviation,

$$-\Delta\delta(0)^T A_r \Delta\delta(0) = k^2_\omega v_{\omega i}^T M v_{\omega i} \quad (30)$$

k_ω is the maximum amplitude of the modal speed deviation. If the inertial control strategy is used, then M is perturbed by a symmetric positive semi-definite matrix. If the maximum speed deviation of the modal variable of the modified system is k'_ω , then

$$-\Delta\delta(0)^T A_r \Delta\delta(0) = k'^2_\omega v_{\omega i}^T (M + \Delta M) v_{\omega i} \quad (31)$$

From (30) and (31) and using the fact that ΔM and M are symmetric positive semi-definite, it can be inferred that

$$k'^2_\omega v_{\omega i}^T M v_{\omega i} \leq k^2_\omega v_{\omega i}^T M v_{\omega i} \quad (32)$$

Hence, it is clear from (32) that by using inertial control, $|k'_\omega| \leq |k_\omega|$ implying either reduction or no change in the relative speed oscillation amplitude for a disturbance like generation or load outage.

IV. PRACTICAL ISSUES IN CONTROLLER DESIGN

(1) Although the control strategies utilize plain proportional control laws, practical controller implementations will require additional blocks like filters, washout circuits and limiters to avoid adverse interactions with the faster neglected dynamics of the plant, remove offsets and ensure that the control order is commensurate with actuator device rating. Some phase compensation also may be required to compensate phase delays

associated with plant and filters, as well as communication delays (in the case of non-local signals). A small phase lag in damping and inertial control may be considered to be beneficial as it introduces synchronizing and damping effects respectively for the oscillatory swing modes.

(2) In practice, the bus phase angles, frequency and rate-of-change of frequency signals may be contaminated by noise, electro-magnetic transients and waveform distortions. In such cases, it may be pragmatic to seek ‘cleaner’ signals which are similar to these quantities, e.g., the speed signals from nearby generators.

(3) Gain selection: While the control strategies discussed earlier fix the controller structure, the selection of the controller gains needs further analysis. The root loci of the overall system for varying gain can be used to select the controller gain as given in [9], [13]. This analysis should consider a detailed model of the power system. The gain may be chosen so that the damping ratio of all controllable modes is higher than a specified target. For this, it is necessary to track the modes which are affected by the controller. This can be done by obtaining the complete eigensolution of the linearized system. However, this may not be feasible for very large systems. Hence, selective eigenvalue analysis of the system may be carried out, wherein only those eigenvalues that are significantly affected by the controller are computed. Algorithms like Subspace Accelerated Dominant Pole Algorithm (SADPA) [14] may be used for this purpose.

Even in the case of gain selection, some useful pointers can be obtained from the circuit analogy discussed in Section II. For example, the gain of the controller can be determined by first obtaining a Thevenin equivalent of the rest of the system at the device terminal(s) from the analogous circuit, and then choosing the ‘resistance’ value based on the maximum power transfer theorem [5].

Eventually, the controller performance for the selected gains has to be cross-verified from a simulation study of the non-linear system for large and small disturbances.

A note about large gain behaviour: The use of eigenvalue sensitivities to analyze is useful only in the understanding of the small-gain behaviour. In a synchronous grid, the emulation of synchronizing effects using symmetric positive semi-definite gain matrices does not affect the structure of the A and M . Hence, increasing the gain simply increases the frequency of the swing modes. The movement is eventually restricted due to the presence of zeros (of the transfer function between power flow and bus phase-angular differences) which are on the imaginary axis and are interleaved with the poles (eigenvalues) associated with the swing modes [8]. A similar effect is expected if inertia is emulated, except that the swing mode frequencies decrease with increasing gain.

The presence of interleaved zeros also means that if damping control is used, then the damping will initially increase with increase in gain (as predicted by the sensitivity formula), but then ‘turn around’ towards a nearby zero. This is consistent with the intuitive analysis given earlier (see point (e) in Section II-A). The movement of the dominant pole can be increased by changing the zero positions, which can be

achieved by using modified signals that compensate the feed-forward effect [8], [13].

V. CASE STUDIES

A. Eigenvalue Movement for the Damping, Synchronizing and Inertial Control laws

The inferences relating to the eigenvalue sensitivities with damping, synchronizing and inertial control strategies are tested on the detailed model of the Indian Grid (adapted from 2015 data). A summary of the component count is given in Table II. The HVdc links selected for testing the control strategies are given below and are also indicated on the map in Fig. 4.

Talcher Kolar link: This link connects from Talcher (rectifier end) to Kolar (inverter end). It has a capacity of 2500 MW at ± 500 kV voltage extending over 1450 km.

Chandrapur Padghe link: This link connects from Chandrapur (rectifier end) to Padghe (inverter end). It has a capacity of 1500 MW at ± 500 kV voltage extending over 752 km.

TABLE II: Grid Components

Components	Number
Buses	7242
Transmission Lines	8729
Transformers	3745
Generators	1232
Wind Generators	18
HVdc Links	9
TCSC	6
SVC	1
Fixed Shunts	1182
Total Load (GW)	116

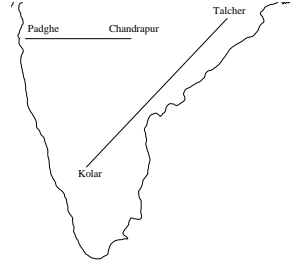


Fig. 4: Selected HVdc links in peninsular India

Results: The power flow of each link is varied in proportion to the phase angular differences, frequencies and rate-of-change of frequencies (one at a time). For example, to introduce the synchronizing effect, the real power transfer through the selected HVdc links are modulated as follows:

$$\Delta P_{tal-kol} = \frac{\Delta \phi_{tal} - \Delta \phi_{kol}}{\mathcal{L}_{tk}} \quad (33)$$

$$\Delta P_{ch-pad} = \frac{\Delta \phi_{ch} - \Delta \phi_{pad}}{\mathcal{L}_{cp}} \quad (34)$$

where $\Delta P_{tal-kol}$ and ΔP_{ch-pad} are the dc link power transfer orders for the Talcher-Kolar and Chandrapur-Padghe HVdc links respectively. $\Delta \phi_{tal}$, $\Delta \phi_{kol}$, $\Delta \phi_{ch}$ and $\Delta \phi_{pad}$ are the phase angular deviations at the Talcher terminal, Kolar terminal, Chandrapur terminal and Padghe terminal respectively. \mathcal{L}_{tk} and \mathcal{L}_{cp} are the gains of the controllers.

Assuming the HVdc links are lossless, the shunt real power injections at the dc terminals are given by

$$\Delta P_{sh(tal)} = -\Delta P_{sh(kol)} = -\Delta P_{tal-kol} \quad (35)$$

$$\Delta P_{sh(ch)} = -\Delta P_{sh(pad)} = -\Delta P_{ch-pad} \quad (36)$$

This implies that

$$\begin{bmatrix} \Delta P_{sh(tal)} \\ \Delta P_{sh(kol)} \\ \Delta P_{sh(ch)} \\ \Delta P_{sh(pad)} \end{bmatrix} = \begin{bmatrix} -\frac{1}{\mathcal{L}_{tk}} & \frac{1}{\mathcal{L}_{tk}} & 0 & 0 \\ \frac{1}{\mathcal{L}_{tk}} & -\frac{1}{\mathcal{L}_{tk}} & 0 & 0 \\ 0 & 0 & -\frac{1}{\mathcal{L}_{cp}} & \frac{1}{\mathcal{L}_{cp}} \\ 0 & 0 & \frac{1}{\mathcal{L}_{cp}} & -\frac{1}{\mathcal{L}_{cp}} \end{bmatrix} \begin{bmatrix} \Delta \phi_{tal} \\ \Delta \phi_{kol} \\ \Delta \phi_{ch} \\ \Delta \phi_{pad} \end{bmatrix} \quad (37)$$

$\Delta P_{sh(tal)}$ and $\Delta P_{sh(kol)}$ represent the shunt injected real power at Talcher (rectifier end) and Kolar (inverter end). Similarly, $\Delta P_{sh(ch)}$ and $\Delta P_{sh(pad)}$ represent the shunt injected real power at Chandrapur (rectifier end) and Padghe (inverter end).

We use SADPA [14] to determine the modes sensitive to this control law. SADPA takes the linearized differential-algebraic model, with power flow as the control input and phase angular difference as the feedback signal. The dominant eigenvalues λ , i.e., those with the largest values of $(|\text{Residue}(\lambda)|/|\text{Re}(\lambda)|)$ are obtained from the algorithm.

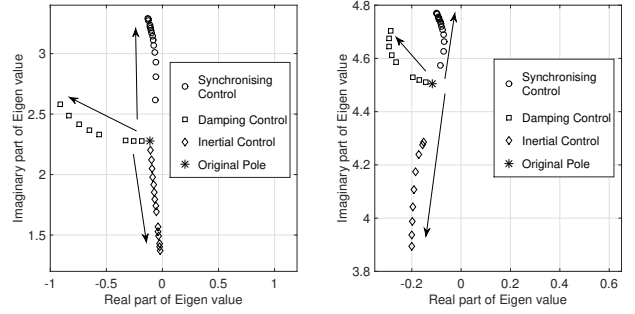


Fig. 5: Most sensitive swing modes of Talcher-Kolar link (independent control)

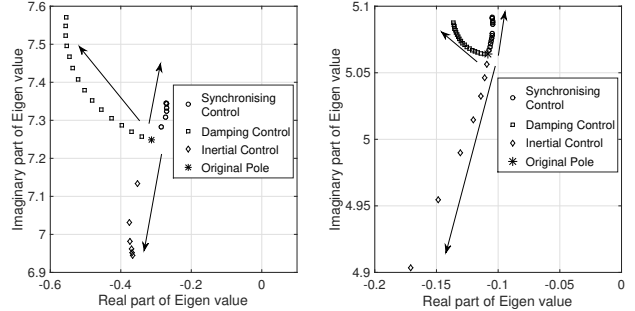


Fig. 6: Most sensitive swing modes of Chandrapur-Padghe link (independent control)

It is found that the two most sensitive modes for the Talcher-Kolar link are around 2.4 rad/s and 4.5 rad/s. The former mode is an important North-South inter-area swing mode in the Indian system and has also been detected using real-life WAMS measurements. The two most sensitive swing modes for the Chandrapur-Padghe link are found to be around 7.25 rad/s and 5.06 rad/s, the latter mode being an East-West Mode.

The root loci of the two most sensitive eigenvalues (mentioned above) are shown in Fig. 5 for the Talcher-Kolar link, and Fig. 6 for Chandrapur-Padghe link. Similar to (37), we have carried out the root loci study for the damping and inertial

strategies, by replacing the phase angle in (37) by frequencies and rate-of-change of frequencies.

The inertial action reduces the swing frequency and the synchronizing action increases the swing frequency monotonically as the gain is increased. This is as anticipated from the analysis of the earlier sections. Although this movement is not exactly vertical due to the fact that detailed models are used here, it is nearly so.

The damping control introduces damping by shifting the mode to the left side for small gains. As the gain is increased, eigenvalues turn back, as anticipated earlier in Section II-A, point (e) and Section IV, point (3).

B. Inertial control using a dc link

The inertial control strategy as discussed in Section III-C, is tested on a three machine system (data adapted from [15]) shown in Fig. 7, with a VSC based dc link connected between bus 6 and 9. The shunt real power injection is modulated in the following strategy:

$$\begin{bmatrix} \Delta P_{sh6} \\ \Delta P_{sh9} \end{bmatrix} = \begin{bmatrix} -C_{69} & C_{69} \\ C_{69} & -C_{69} \end{bmatrix} \frac{d}{dt} \begin{bmatrix} \Delta \omega_{b6} \\ \Delta \omega_{b9} \end{bmatrix} \quad (38)$$

ΔP_{sh6} and ΔP_{sh9} are the shunt power injections at bus 6 (rectifier terminal) and bus 9 (inverter terminal) of the network respectively. $\Delta \omega_{b6}$ and $\Delta \omega_{b9}$ are the bus frequency deviations at bus 6 and bus 9 respectively and C_{69} is the gain of the controller.

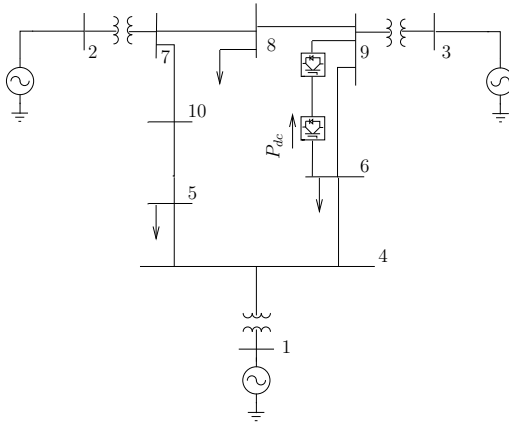


Fig. 7: Three machine system

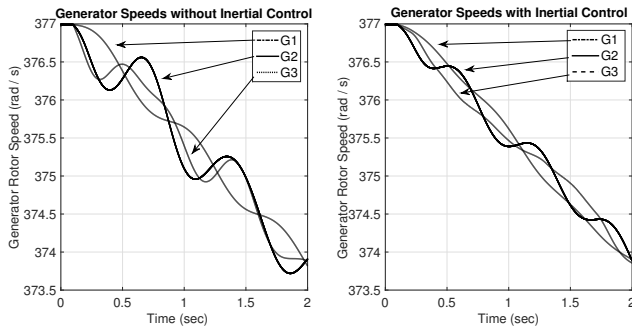


Fig. 8: Response of Generator speeds for HVdc Inertial Control

This strategy will not affect the centre-of-inertia motion (since the overall load-generation balance is not affected if we neglect the losses in the HVdc link), but is expected to reduce the relative speed deviations as predicted in Section III-D. Since generator rotor speeds consist of *both* swing modes and centre-of-inertia motion components, there is some merit in seeking to reduce the relative speed oscillations through this inertial strategy. The use of local rate-of-change of frequency is avoided, since bus voltages are prone to noise and distortion. The disturbance considered is a 20% increase of load at bus 8 at 0.1 sec. It can be seen from Fig. 8 that there is reduction in amplitude of relative speed excursions of the generators with the control strategy mentioned above. There is also reduction in the initial rate-of-change of the individual generator speeds.

VI. CONCLUSION

This paper has presented a generalized analysis of the effects of the introduction of damping, synchronizing and inertial effects using a circuit analogy of the electro-mechanical system as well as eigenvalue sensitivity analysis. The differential-algebraic formulation of system equations facilitates a unified analysis of these effects. The effects of these strategies are characterized in terms of eigenvalue sensitivities. The control strategies are independent of size of the network, topology, number of generators and operating condition. The inferences drawn from the analysis presented in this paper are illustrated with a case study on a large, realistic power grid.

VII. ACKNOWLEDGEMENTS

The authors would like to thank Vedanta Pradhan and Ajinkya Sinkar of IIT Bombay for their assistance in carrying out the case studies.

APPENDIX A

GENERALIZED EIGENVALUE SENSITIVITY EXPRESSIONS

Consider a linear system governed by the equation

$$\mathcal{M}\dot{x} = \mathcal{A}x \quad (39)$$

Let λ_i be the eigenvalue and the corresponding left and right eigenvectors are u_i and v_i respectively. Let $(u_i)_k$ represents the k^{th} entry of u_i and $(v_i)_l$ represents the l^{th} entry of v_i .

$$\mathcal{A}v_i = \lambda_i \mathcal{M}v_i \quad (40)$$

$$u_i^T \mathcal{A} = \lambda_i u_i^T \mathcal{M} \quad (41)$$

A. Perturbation in Matrix \mathcal{A}

Let Δa_{kl} denote a small perturbation in $\mathcal{A}(k, l)$. Differentiating (40) w.r.t. a_{kl} and proceeding as in [16], we get

$$\frac{\partial \mathcal{A}}{\partial a_{kl}} v_i + \mathcal{A} \frac{\partial v_i}{\partial a_{kl}} = \frac{\partial \lambda_i}{\partial a_{kl}} \mathcal{M}v_i + \lambda_i \mathcal{M} \frac{\partial v_i}{\partial a_{kl}} \quad (42)$$

Pre-multiplying by u_i^T , we get

$$u_i^T \frac{\partial \mathcal{A}}{\partial a_{kl}} v_i + u_i^T \mathcal{A} \frac{\partial v_i}{\partial a_{kl}} = u_i^T \frac{\partial \lambda_i}{\partial a_{kl}} \mathcal{M}v_i + \lambda_i u_i^T \mathcal{M} \frac{\partial v_i}{\partial a_{kl}} \quad (43)$$

Using (41), the expression for eigenvalue sensitivity is

$$\frac{\partial \lambda_i}{\partial a_{kl}} = \frac{(u_i)_k (v_i)_l}{u_i^T \mathcal{M} v_i} \quad (44)$$

Using linear perturbation analysis, the perturbation in the eigenvalue λ_i due to a perturbation $\Delta \mathcal{A}$ in \mathcal{A} is

$$\Delta \lambda_i = \frac{u_i^T \Delta \mathcal{A} v_i}{u_i^T \mathcal{M} v_i} \quad (45)$$

B. Perturbation in Matrix \mathcal{M}

Let Δm_{kl} denote a small perturbation in $\mathcal{M}(k, l)$. Differentiating (40) w.r.t. m_{kl} and proceeding as in [16], we get

$$\mathcal{A} \frac{\partial v_i}{\partial m_{kl}} = \frac{\partial \lambda_i}{\partial m_{kl}} \mathcal{M} v_i + \lambda_i \frac{\partial \mathcal{M}}{\partial m_{kl}} v_i + \lambda_i \mathcal{M} \frac{\partial v_i}{\partial m_{kl}} \quad (46)$$

Pre-multiplying by u_i^T , we get

$$u_i^T \mathcal{A} \frac{\partial v_i}{\partial m_{kl}} = \frac{\partial \lambda_i}{\partial m_{kl}} u_i^T \mathcal{M} v_i + \lambda_i u_i^T \frac{\partial \mathcal{M}}{\partial m_{kl}} v_i + \lambda_i u_i^T \mathcal{M} \frac{\partial v_i}{\partial m_{kl}} \quad (47)$$

Using (41), the expression for eigenvalue sensitivity is

$$\frac{\partial \lambda_i}{\partial m_{kl}} = -\lambda_i \frac{(u_i)_k (v_i)_l}{u_i^T \mathcal{M} v_i} \quad (48)$$

Using linear perturbation analysis, the perturbation in the eigenvalue λ_i due to a perturbation $\Delta \mathcal{M}$ in \mathcal{M} is

$$\Delta \lambda_i = -\lambda_i \frac{u_i^T \Delta \mathcal{M} v_i}{u_i^T \mathcal{M} v_i} \quad (49)$$

REFERENCES

- [1] A. G. Phadke and J. S. Thorp, *Synchronized Phasor Measurements and their Applications*. Springer, New York, 2008.
- [2] J. S. Thorp, C. E. Seyler, and A. G. Phadke, "Electromechanical wave propagation in large electric power systems," *IEEE Transactions on Circuits and Systems I: Fundamental Theory and Applications*, vol. 45, no. 6, pp. 614–622, Jun 1998.
- [3] O. Samuelsson, "Load modulation for damping of electro-mechanical oscillations," in *2001 IEEE Power Engineering Society Winter Meeting. Conference Proceedings (Cat. No.01CH37194)*, vol. 1, Jan 2001, pp. 241–246 vol.1.
- [4] M. Singh, A. Allen, E. Muljadi, and V. Gevorgian, "Oscillation damping: A comparison of wind and photovoltaic power plant capabilities," in *2014 IEEE Symposium on Power Electronics and Machines for Wind and Water Applications*, July 2014, pp. 1–7.
- [5] M. R. S. Tirtashi, O. Samuelsson, and J. Svensson, "Impedance matching for vsc-hvdc and energy storage damping controllers," *IEEE Transactions on Power Delivery*, vol. PP, no. 99, pp. 1–1, 2017.

- [6] P. Agnihotri, A. M. Kulkarni, and A. M. Gole, "Robust global control strategies for improvement of angular stability using facts and hvdc devices," *International Journal of Emerging Electric Power Systems*, vol. 14, no. 1, pp. 95–104, 2013.
- [7] T. Smed and G. Andersson, "Utilizing hvdc to damp power oscillations," *IEEE Transactions on Power Delivery*, vol. 8, no. 2, pp. 620–627, 1993.
- [8] U. P. Mhaskar and A. M. Kulkarni, "Power oscillation damping using facts devices: modal controllability, observability in local signals, and location of transfer function zeros," *IEEE Transactions on Power Systems*, vol. 21, no. 1, pp. 285–294, Feb 2006.
- [9] P. Agnihotri, A. M. Kulkarni, A. M. Gole, B. A. Archer, and T. Weekes, "A robust wide-area measurement-based damping controller for networks with embedded multiterminal and multiinfeed hvdc links," *IEEE Transactions on Power Systems*, vol. 32, no. 5, pp. 3884–3892, Sept 2017.
- [10] K. R. Padiyar, *Structure preserving energy functions in power systems: theory and applications*. CRC Press, 2013.
- [11] P. Kundur, *Power system stability and control*. McGraw-Hill, 1994.
- [12] D. S. Watkins, *Fundamentals of matrix computations*. John Wiley & Sons, 2004, vol. 64.
- [13] E. V. Larsen, J. J. Sanchez-Gasca, and J. H. Chow, "Concepts for design of facts controllers to damp power swings," *IEEE Transactions on Power Systems*, vol. 10, no. 2, pp. 948–956, May 1995.
- [14] J. Rommes and N. Martins, "Efficient computation of transfer function dominant poles using subspace acceleration," *IEEE Transactions on Power Systems*, vol. 21, no. 3, pp. 1218–1226, Aug 2006.
- [15] P. M. Anderson and A. A. Fouad, *Power system control and stability*. John Wiley & Sons, 2008.
- [16] B. Porter and R. Crossley, *Modal Control: Theory and Applications*. Taylor & Francis Group, 1972.

Kaustav Dey received his B.E. degree in Electrical Engineering from Jadavpur University, India in 2015. He is currently a Ph.D student of Power Electronics and Power Systems, Department of Electrical Engineering at the Indian Institute of Technology, Bombay. His research interests include Power system dynamics, HVdc and applications of signal processing in power system.

P. Agnihotri (S'09) received his B.E. degree in electronics and communication engineering from the Rajiv Gandhi Technical University, India in 2007. He obtained his M.S. degree in electrical engineering in 2010 from University of North Dakota and his PhD in 2016 from the University of Manitoba, Canada. His research interests include Power system dynamics, HVDC and FACTS.

A. M. Gole (M'82, SM', F'10) received the B.Tech. degree in electrical engineering from the Indian Institute of Technology, Bombay, India, in 1978 and the Ph.D. degree from the University of Manitoba, Winnipeg, MB, Canada, in 1982. He holds the Natural Sciences and Engineering Research Council of Canadas (NSERC) Industrial Research Chair in Power Systems Simulation at the University of Manitoba. Dr. Gole is active with CIGRE and IEEE working groups and was the 2007 recipient of the IEEE PES Nari Hingorani FACTS Award.

A. M. Kulkarni (M'07) received his B.E. degree in electrical engineering from the University of Roorkee in 1992. He obtained his M.E. degree in electrical engineering in 1994 and his PhD in 1998 from the Indian Institute of Science, Bangalore. He is a Professor at the Indian Institute of Technology, Bombay. His research interests include Power system dynamics, HVdc and FACTS.